Electronic Supplementary Material (ESI) for Journal of Materials Chemistry A.

Supporting Information

Unveiling highly ambient-stable multilayered 1T-MoS$_2$ towards all-solid-state flexible supercapacitors

Xin Wang[a,b,‡], Wei Ding[a,b,‡], Han Li[a,b], Hui Li[a,b], Shunjin Zhu[a,b], Xiaoguang Zhu[a], Jianming Dai[a],

Zhigao Sheng[c], Hai Wang[d], Xuebin Zhu[a*], Yuping Sun[a,c,e*] & Shi Xue Dou[f]

[a] Key Laboratory of Materials Physics, Institute of Solid State Physics, Chinese Academy of

Sciences, Hefei 230031, People's Republic of China

[b] University of Science and Technology of China, Hefei 230026, People's Republic of China

[c] High Magnetic Field Laboratory, Chinese Academy of Sciences, Hefei 230031, People's

Republic of China

[d] Key Laboratory of New Processing Technology for Nonferrous Metals and Materials, Ministry

of Education, Guilin University of Technology, Guilin 541004, People's Republic of China

[e] Collaborative Innovation Center of Advanced Microstructures, Nanjing University, Nanjing

210093, People's Republic of China

[f] Institute for Superconducting and Electronic Materials, University of Wollongong, NSW 2500,

Australia

E-mail: XZ (xbzhu@issp.ac.cn); YS (ypsun@issp.ac.cn)

Experimental Methods

Samples Preparation

Preparation of 2H-MoS$_2$ Nanosheets. (NH$_4$)$_6$Mo$_7$O$_{24}$·4H$_2$O (CAS number 12027-67-7) and thiourea (CAS number 62-56-6) were purchased from Alfa Aesar. All chemicals were used without any further purification. 1.4209 g thiourea and 0.7242 g (NH$_4$)$_6$Mo$_7$O$_{24}$·4H$_2$O were dissolved in deionized water (21.8 mL) and stirred vigorously for 30 min to get a homogeneous solution. After the mixture was transferred to a Teflon-lined stainless-steel autoclave (28mL capacity). Then, it was heated to 210℃ in 40 min and kept for 18 h. The resulting product was filtered, washed several times by deionized water and ethanol, and finally dried at 70℃ in a vacuum oven.

Preparation of MoS$_2$-CTAB Nanosheets. Thiourea and (NH$_4$)$_6$Mo$_7$O$_{24}$·4H$_2$O were dissolved in deionized water and stirred vigorously to get a homogeneous solution. After the mixture was transferred to a Teflon-lined stainless-steel autoclave (the usage was the same as that aforementioned). 0.35 g of CTAB was further added to the solution under constant stirring. Then, the following experimental procedure is consistent with the synthesis of 2H-MoS$_2$

Preparation of 1T-MoS$_2$ Nanosheets. Thiourea and (NH$_4$)$_6$Mo$_7$O$_{24}$·4H$_2$O were dissolved in deionized water and stirred vigorously to get a homogeneous solution. After the mixture was transferred to a Teflon-lined stainless-steel autoclave (the usage is consistent with the synthesis of 2H-MoS$_2$). Then, it was heated to 210℃ in 40 min and kept for 18 h, a magnetic field (H=9T) was applied at the same time. After synthesis, when the temperature was decreased to 80 °C, the magnetic field was then removed and the reaction system was naturally cooled to room temperature. After that, the following experimental procedure is consistent with the synthesis of 2H-MoS$_2$.

Materials Characterizations

Microstructure characterizations were conducted by X-ray diffraction (XRD) patterns (Philips X′pert PRO X-ray diffractometer with Cu K radiation, λ = 0.15406 nm), Field emission scanning electron microscope (FE-SEM, Quanta 200FEG) and Energy-dispersive X-ray spectroscopy (EDX, Oxford EDX, with INCA software), transmission electron microscope (TEM, JEM-2100) with configured EDX, Raman spectroscopy was carried out by a LabRAMHR800 UV NIR spectrometer with 532 nm laser excitation. The PL spectra were obtained with a Nd:YAG laser (λ = 532 nm). Contact angle measurements of water were performed at room temperature using the

sessile drop technique. The water drops were placed on the surface of cold-pressed 2H-MoS$_2$, MoS$_2$-CTAB and 1T-MoS$_2$ discs. The contact angles were measured from photographs taken with a CCD camera yielding an accuracy of approximately ±2°.

Electrochemical measurements and Evaluations

For the electrochemical tests of 2H-MoS$_2$, MoS$_2$-CTAB, 1T-MoS$_2$ electrodes, the working electrodes in a three-electrode configuration were fabricated as followings: a mixture of active material (2H-MoS$_2$, MoS$_2$-CTAB or 1T-MoS$_2$), polyvinylidene fluoride (PVDF) and carbon black with a weight ratio of 8: 1: 1 was uniformly cast on carbon papers. The conductivity of the carbon paper (Toray, Japan) can reach ~ 17 240 S m^{-1}. The area of the working electrodes is ~1 cm^2, and the mass of loading of electrodes is ~ 2 mg. Then the electrodes were dried in vacuum oven at 45 °C for 12 hours. Platinum and Ag/AgCl in 1 M KCl were used as the counter electrode and reference electrode, respectively. The gravimetric specific capacitance calculated from from the galvanostatic charge-discharge (GCD) curves is given by:

$$C = jt/\Delta V \tag{1}$$

and it calculated from the cyclic voltammetry (CV) curves is given by:

$$C = \frac{1}{\Delta V} \int \frac{jdV}{v} \tag{2}$$

where C is the specific capacitance (F g^{-1}), ΔV is the potential window (V), v is the scan rate (V s^{-1}), V is the potential (V), j is the current density (A g^{-1}), and t is time (s). Electrochemical impedance spectroscopy (EIS) was performed with open circuit voltage in frequency range of 100 kHz to 0.01 Hz. All tests were performed using the CHI 660E electrochemical work station in 1 M Na$_2$SO$_4$, 1 M Li$_2$SO$_4$ and 1 M H$_2$SO$_4$ electrolyte.

Preparation of PVA-Na$_2$SO$_4$ gel: Firstly, 1 g of polyvinyl alcohol (PVA) powder was dissolved into 10 mL of DI water, and the mixture was heated to 90°C under exquisite stirring until the solution became clear and cool to room temperature. Then, 5 mL aqueous Na$_2$SO$_4$ (1 M) was added dropwise into the above solution under constant stirring. To prepare the flexible electrodes, uniformly apply 1T-MoS$_2$ slurry on a flexible carbon cloth and then dried in a blast drying oven at 45°C for 12h. Subsequently, two 1T-MoS$_2$ flexible electrodes which are coated with PVA-Na$_2$SO$_4$ gel were assembled into a supercapacitor by sandwiching cellulose membrane as separator

between them. After the PVA-Na_2SO_4 gel solidified at room temperature for ~12 h, the symmetric flexible all-solid-state supercapacitor (ASSS) was obtained.

The areal specific capacitance of the device based on area of the active material was calculated from charge-discharge curves according to the following equation:

$$C = \frac{I \times \Delta t}{S \times \Delta V}$$
(3)

where I is the constant discharge current (A); Δt is the time for a full discharge (s); S is the facing area of the active material on the two working electrodes (cm^2); and ΔV is the voltage drop on discharge (V). The areal energy densities ($E = \mu Wh\ cm^{-2}$) and power densities ($P = \mu W\ cm^{-2}$) of the ASSS device were calculated using the following equations:

$$E = 1/(2 \times 3.6) \times C \times \Delta V^2$$
(4)

$$P = 3600 \times E/\Delta t$$
(5)

where C is the areal specific capacitance of the ASSS device, ΔV is the potential window during the discharging process, Δt is the time for a full discharge of device. The CV, GCD and cyclic stability tests of ASSS devices assembled with 1T-MoS_2 as electrodes were performed using the CHI 660E electrochemical work station.
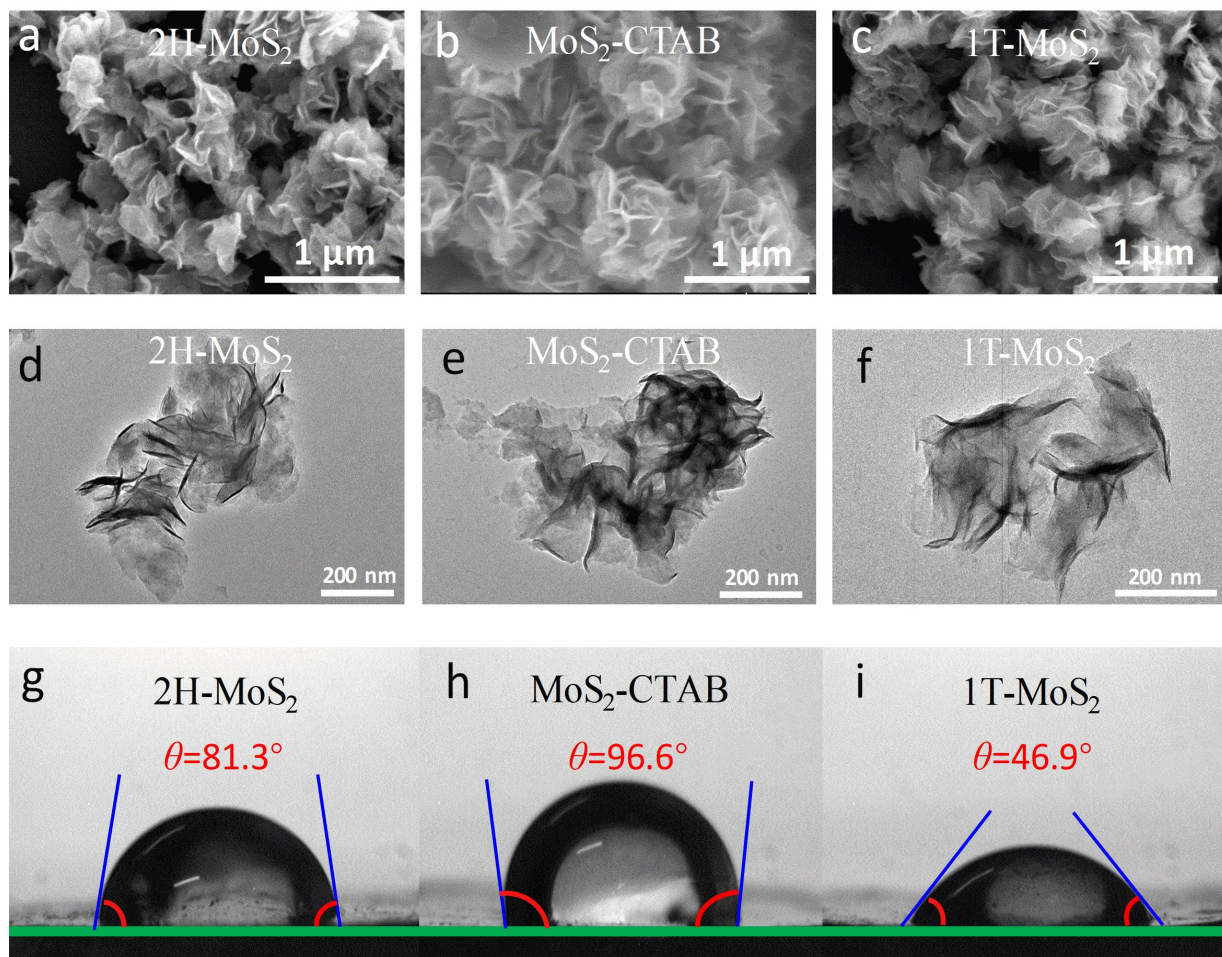
Figure S1. Microstructure and hydrophilic results of three types of MoS$_2$ samples. (a-c) FE-SEM images, (d-f) TEM images, (e-g) static contact angle images of 2H-MoS$_2$, MoS$_2$-CTAB, 1T-MoS$_2$ nanosheets, respectively.
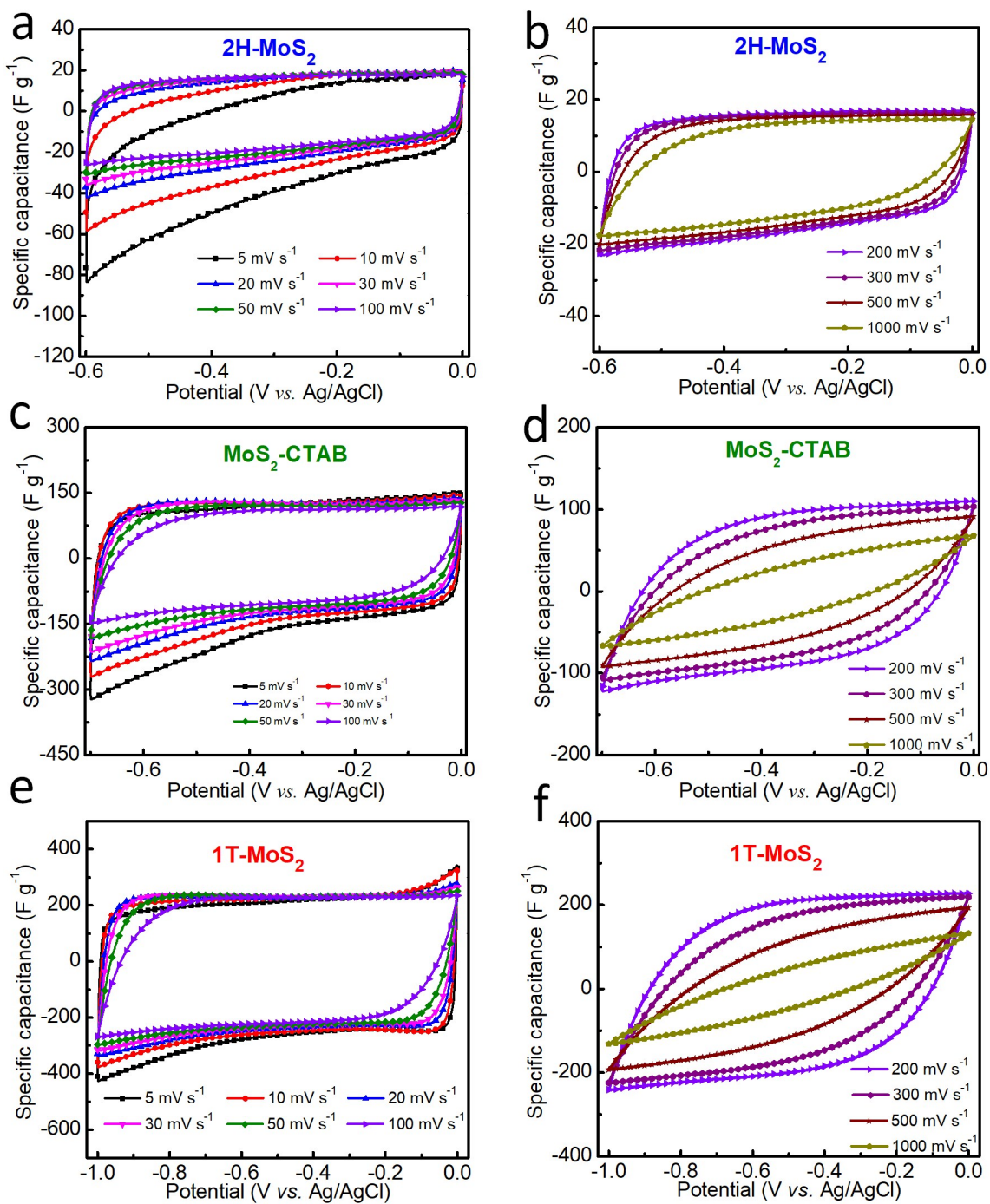
Figure S2. CV curves at different scan rates (5-1 000 mV s^{-1}) of three types of MoS$_2$ samples. (a), (b) 2H-MoS$_2$, (c), (d) MoS$_2$-CTAB, (e), (f) 1T-MoS$_2$ electrode.
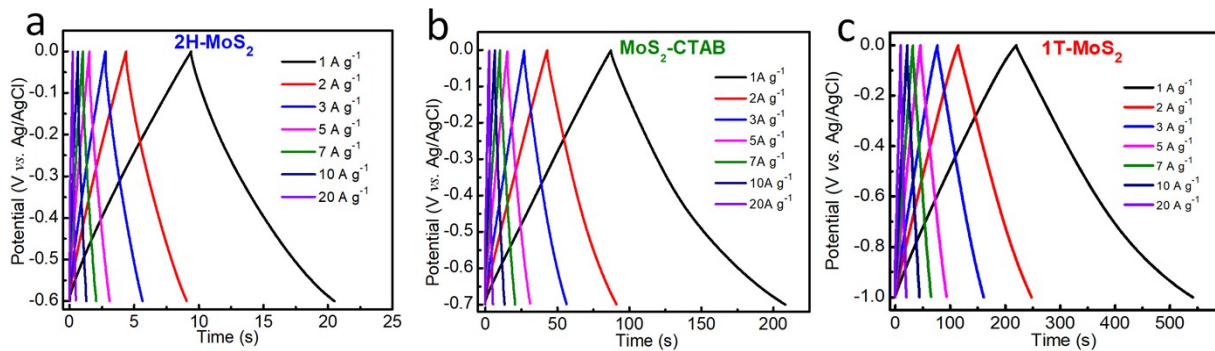
Figure S3. GCD curves at different current densities (1-20 A g^{-1}) of three types of MoS$_2$ samples. (a), 2H-MoS$_2$, (b) MoS$_2$-CTAB, (c) 1T-MoS$_2$ electrode.

$IR_{drop}=0.00925I+0.00069$

$IR_{drop}=0.00751I+0.00163$

$IR_{drop}=0.00559I+0.00104$
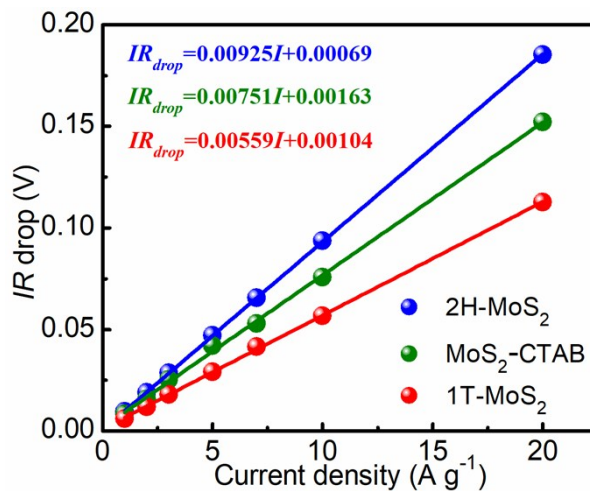
Figure S4. Potential drop associated with the IR drops of 2H-MoS$_2$, MoS$_2$-CTAB, 1T-MoS$_2$ electrode *vs.* different discharge current densities.
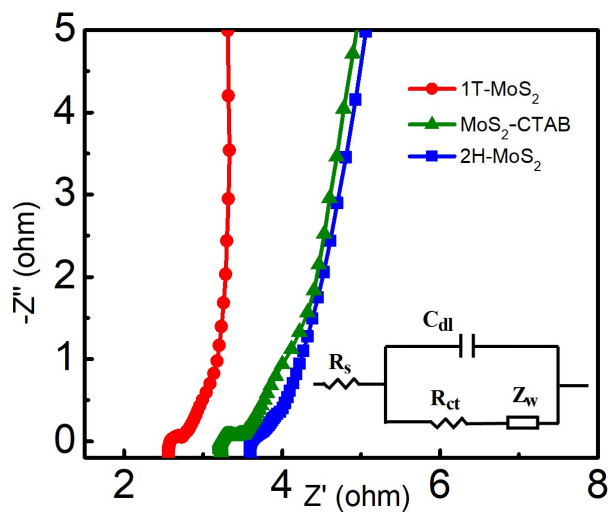
Figure S5. Comparisons of Nyquist plots of the 2H-MoS$_2$, MoS$_2$-CTAB, 1T-MoS$_2$ electrodes in 1 M Na$_2$SO$_4$.
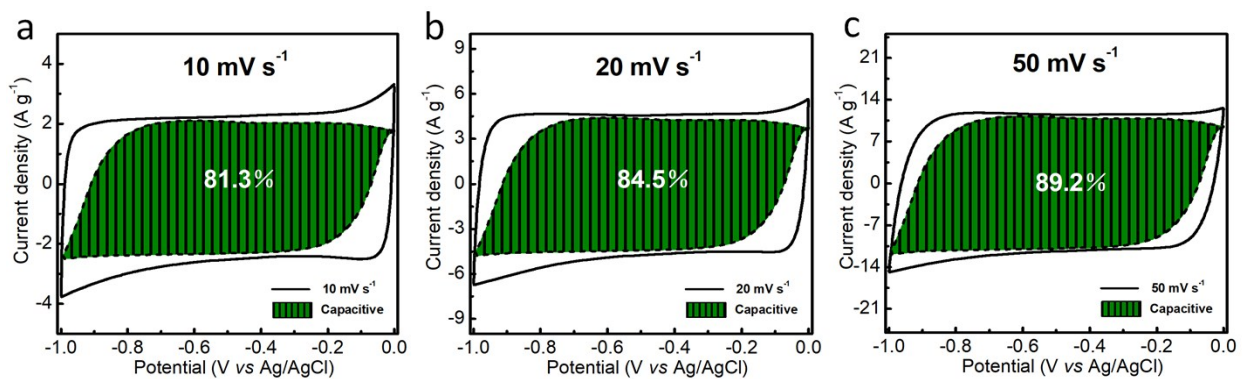
Figure S6. Kinetics and quantitative analysis of the 1T-MoS$_2$ electrodes in 1 M Na$_2$SO$_4$. Capacitive (green) contribution to charge storage of 1T-MoS$_2$ electrode at 10, 20, and 50 mV s^{-1}.
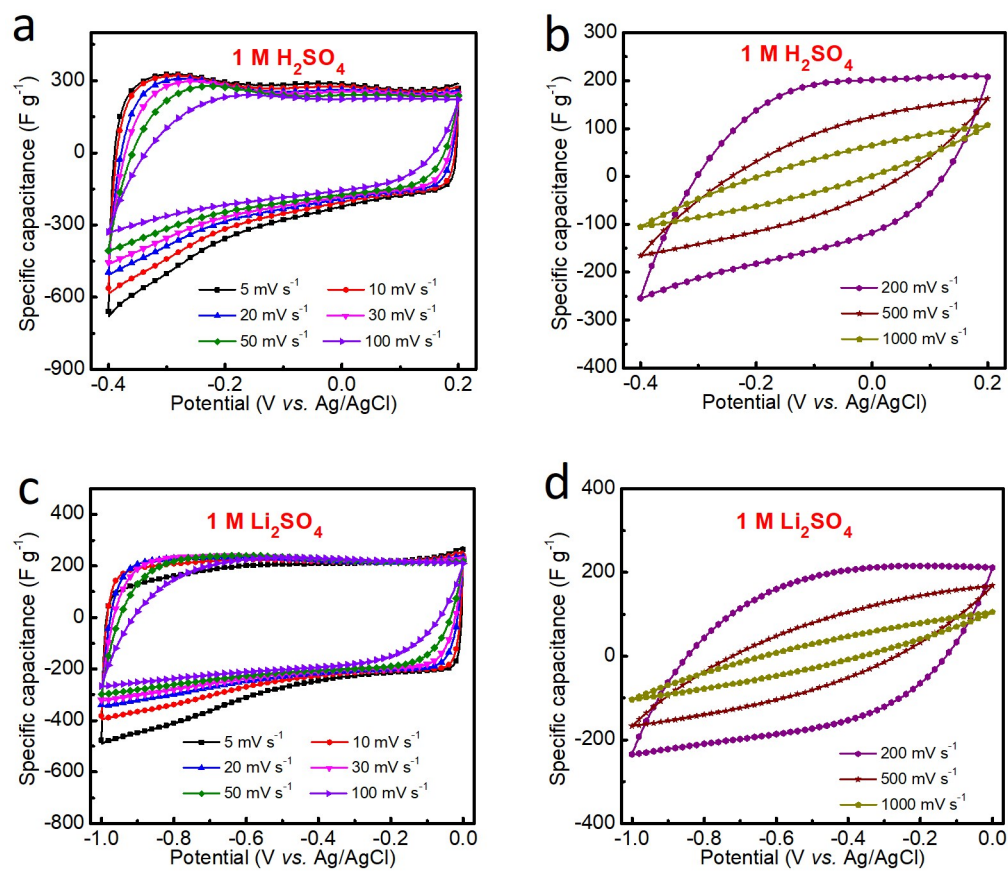
Figure S7. CV curves at different scan rates (5-1000 mV s^{-1}) of 1T-MoS$_2$ electrodes in 1 M H$_2$SO$_4$ (a), (b) and 1 M Li$_2$SO$_4$ (c), (d).
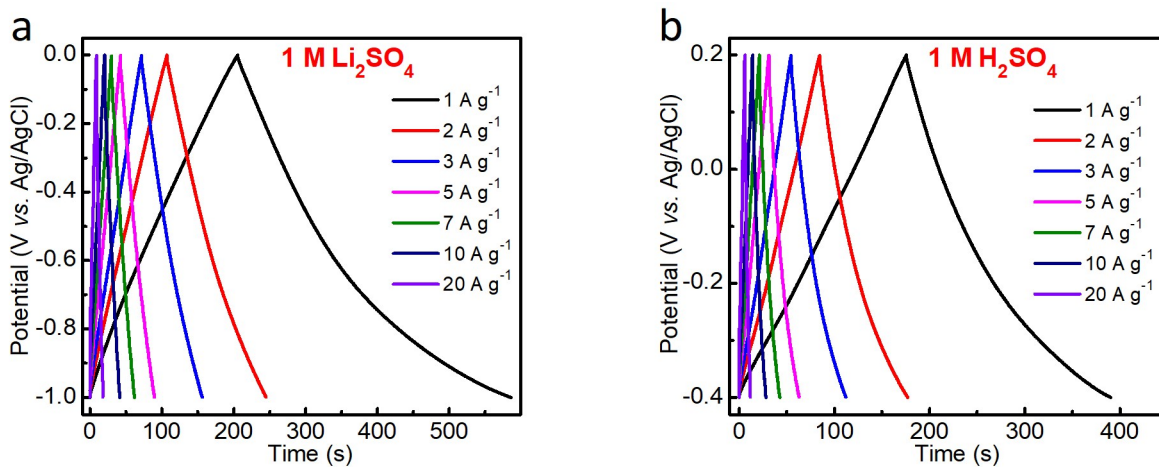
Figure S8. GCD curves at different current densities (1-20 A g^{-1}) of 1T-MoS$_2$ electrodes in 1 M Li$_2$SO$_4$ (a) and 1 M H$_2$SO$_4$ (b).
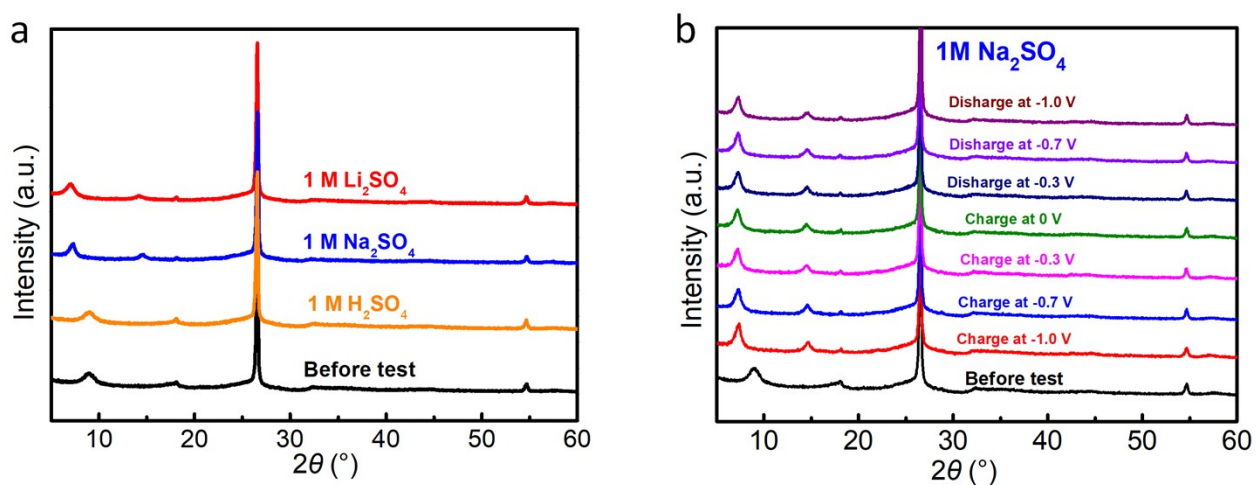
Figure S9. *Ex-situ* XRD patterns of 1T-MoS$_2$ electrodes. (a) XRD patterns of 1T-MoS$_2$ cycled 1T-MoS$_2$ electrodes in different sulphate-based electrolytes: Li$_2$SO$_4$ (red), Na$_2$SO$_4$ (blue), H$_2$SO$_4$ (orange). (b) *Ex-situ* XRD patterns of 1T-MoS$_2$ electrode during electrochemical charge-discharge in 1 M Na$_2$SO$_4$.
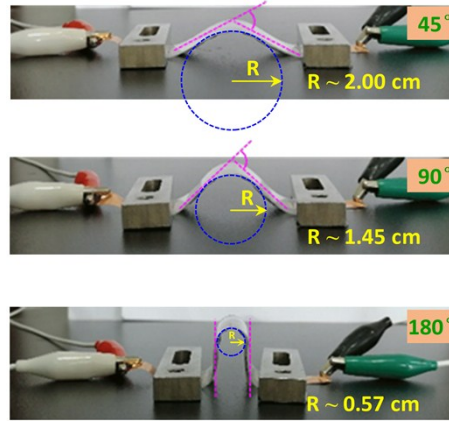
Figure S10. Digital photographs and values of R (the bending radius of curvature) of flexible 1T-MoS₂ based all-solid-state flexible supercapacitor bended at different angles.
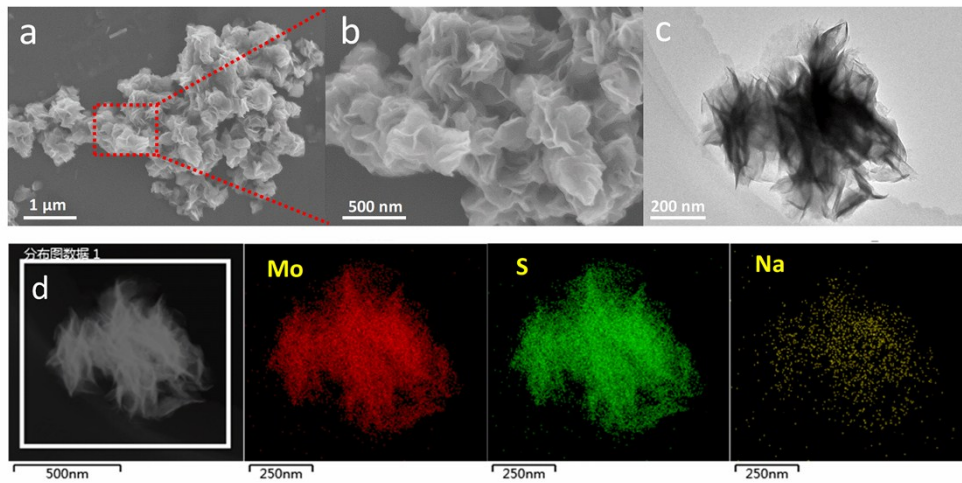

Figure S11. (a, b) SEM images, (c) TEM image and (d) corresponding elemental mapping images of Mo, S and Na elements of 1T-MoS$_2$ after long-term cycled.

Table S1. Specific capacitances of 2H-MoS$_2$, MoS$_2$-CTAB and 1T-MoS$_2$ electrodes at 1 A g^{-1}, 2 A g^{-1}, 3 A g^{-1}, 5 A g^{-1}, 7 A g^{-1}, 10 A g^{-1} and 20 A g^{-1} in 1 M Na$_2$SO$_4$ electrolyte.

Sample	1 A g^{-1}	2 A g^{-1}	3 A g^{-1}	5 A g^{-1}	7 A g^{-1}	10 A g^{-1}	20 A g^{-1}
2H-MoS$_2$	20 F g^{-1}	18 F g^{-1}	16 F g^{-1}	14 F g^{-1}	13 F g^{-1}	12 F g^{-1}	9 F g^{-1}
MoS$_2$-CTAB	173 F g^{-1}	137 F g^{-1}	128 F g^{-1}	114 F g^{-1}	105 F g^{-1}	98 F g^{-1}	74 F g^{-1}
1T-MoS$_2$	320 F g^{-1}	264 F g^{-1}	255 F g^{-1}	247 F g^{-1}	236 F g^{-1}	224 F g^{-1}	202 F g^{-1}

Table S2. Specific capacitances of 1T-MoS$_2$ electrodes at 1 A g^{-1}, 2 A g^{-1}, 3 A g^{-1}, 5 A g^{-1}, 7 A g^{-1}, 10 A g^{-1} and 20 A g^{-1} in 1 M Li$_2$SO$_4$, H$_2$SO$_4$ and Na$_2$SO$_4$ electrolytes, respectively.

Sample	1 A g^{-1}	2 A g^{-1}	3 A g^{-1}	5 A g^{-1}	7 A g^{-1}	10 A g^{-1}	20 A g^{-1}
1 M Li$_2$SO$_4$	379 F g^{-1}	274 F g^{-1}	251 F g^{-1}	232 F g^{-1}	222 F g^{-1}	210 F g^{-1}	183 F g^{-1}
1 M H$_2$SO$_4$	358 F g^{-1}	310 F g^{-1}	286 F g^{-1}	264 F g^{-1}	249 F g^{-1}	230 F g^{-1}	193 F g^{-1}
1 M Na$_2$SO$_4$	320 F g^{-1}	264 F g^{-1}	255 F g^{-1}	247 F g^{-1}	236 F g^{-1}	224 F g^{-1}	202 F g^{-1}

Table S3. Comparisons of cycling stability, energy and power density of all-solid-state flexible symmetric supercapacitors (ASSS) with ASSS devices reported recently.

ASSS devices	Retention	Energy density power density	Refs.
1T-MoS$_2$//1T-MoS$_2$	97.3% and 84.1% after 10000, 30000 cycles at 20 mA cm^{-2}, respectively	43.1 μWh cm^{-2} at 500 μW cm^{-2} 17.3 μWh cm^{-2} at 10270 μW cm^{-2}	This work
Ti$_3$C$_2$T$_x$//Co-Al-LDHs	92% after 10000 cycles at 1.25 mA cm^{-2}	8.84 μWh cm^{-2} at 230 μW cm^{-2}	[71]
ZnCo$_2$O$_4$/H:ZnO NRs//AC	/	10.1 μWh cm^{-2} at 1750 μWh cm^{-2} 8.7 μWh cm^{-2} at 2640 μWh cm^{-2} 7.2 μWh cm^{-2} at 3250 μWh cm^{-2}	[72]
140-PEDOT//140-PEDOT	/	48.3 μWh cm^{-2} at 220 μW cm^{-2}; 19.1 μWh cm^{-2} at 16800 μW cm^{-2}	[73]
Cu(OH)$_2$/Cu-plated carbon cloth//AC/ carbon cloth	90.8% after 5000 cycles at 5 mA cm^{-2}	49 μWh cm^{-2} at 600 μW cm^{-2}	[74]
THAQ/rGo@PF// THAQ/rGo@PF	81.8% after 2000 cycles at 1 mA cm^{-2}	17.0 μWh cm^{-2} at 164 μW cm^{-2}	[75]
polyaniline-polyvinyl alcohol hydrogel (PPH)// PPH	90% after 1000 cycles at 2.5 A g^{-1}	27.2 μWh cm^{-2} at 200 μW cm^{-2}	[76]
Cu(OH)$_2$/Cu/Dacron// CNF/Dacron	86.4% after 3000 cycles at 50 mV s^{-1}	36 μWh cm^{-2} at 600 μW cm^{-2}	[77]
RGO/MnO$_2$//RGO paper	93% after 2100 cycles at 0.5 A g^{-1}	35.1 μWh cm^{-2} at 37.5 μW cm^{-2}	[78]
GNFs/PNTs// GNFs/PNTs	81% after 5000 cycles at 1.8 mA cm^{-2}	11.4 μWh cm^{-2} at 720 μW cm^{-2}	[79]
MnO$_2$/NiO/indium tin oxides/polyethylene terephthalate//Fe$_2$O$_3$/indium tin oxides/polyethylene terephthalate	89.3% after 10000 cycles	9.6 μWh cm^{-2} at 28.9 μW cm^{-2} 5.6 μWh cm^{-2} at 1680 μW cm^{-2}	[80]
rGO/V$_2$O$_5$-rGO//rGO	≥ 85% after 8000 cycles at 0.25 A g^{-1}	8.1 μWh cm^{-2} at 4170 μW cm^{-2}	[81]
CNT@ MnO$_2$//CNT@PPy	80% after 5000 cycles	18.9 μWh cm^{-2} at 450 μW cm^{-2}	[82]
cotton-derived carbon cloth//MnO$_2$/cotton-derived carbon cloth	87.7% after 5000 cycles	30.1 μWh cm^{-2} at 150 μW cm^{-2} 5.8 μWh cm^{-2} at 7500 μW cm^{-2}	[83]